Original Article
CD4+ T cell exhaustion leads to adoptive transfer therapy failure which can be prevented by immune checkpoint blockade

Jinfei Fu[1,2*], Anze Yu[1,3*], Xiang Xiao[1,4], Juyu Tang[2], Xiongbing Zu[3], Wenhao Chen[1,4], Bin He[1,5]

[1]Immunobiology & Transplant Science Center, Department of Surgery, Houston Methodist Research Institute & Institute for Academic Medicine, Houston Methodist Hospital, Houston, TX 77030, USA; [2]Department of Hand and Microsurgery, Xiangya Hospital of Central South University, Changsha 410008, Hunan, China; [3]Department of Urology, Xiangya Hospital of Central South University, Changsha 410008, Hunan, China; [4]Department of Surgery, Weill Cornell Medicine, Cornell University, New York, NY10065, USA; [5]Department of Medicine-Cancer Biology, Weill Cornell Medicine, Cornell University, New York, NY10065, USA. *Equal contributors.

Abstract: Cytotoxic CD8+ T cell exhaustion is one of the mechanisms underlying the tumor immune escape. The paradigm-shifting immune checkpoint therapy can mitigate CD8+ T lymphocyte exhaustion, reinvigorate the anti-cancer immunity, and achieve durable tumor regression for some patients. Emerging evidence indicates that CD4+ T lymphocytes also have a critical role in anticancer immunity, either by directly applying cytotoxicity toward cancer cells or as a helper to augment CD8+ T cell cytotoxicity. Whether anticancer CD4+ T lymphocytes undergo exhaustion during immunotherapy of solid tumors remains unknown. Here we report that melanoma antigen TRP-1/gp75-specific CD4+ T lymphocytes exhibit an exhaustion phenotype after being adoptively transferred into mice bearing large subcutaneous melanoma. Exhaustion of these CD4+ T lymphocytes is accompanied with reduced cytokine release and increased expression of inhibitory receptors, resulting in loss of tumor control. Importantly, we demonstrate that PD-L1 immune checkpoint blockade can prevent exhaustion, induce proliferation of the CD4+ T lymphocytes, and consequently prevent tumor recurrence. Therefore, when encountering an excessive amount of tumor antigens, tumor-reactive CD4+ T lymphocytes also enter the exhaustion state, which can be prevented by immune checkpoint blockade. Our results highlight the importance of tumor-specific CD4+ T lymphocytes in antitumor immunity and suggest that the current immune checkpoint blockade therapy may achieve durable anticancer efficacy by rejuvenating both tumor antigen-specific CD8+ T lymphocytes and CD4+ T lymphocytes.

Keywords: CD4+ T cells, exhaustion, adoptive transfer therapy, immune checkpoint blockade

Introduction

T lymphocytes are critical in adoptive immunity against infection and cancer. Adult human body contains about 4×10^{11} T lymphocytes. Upon antigen exposure, a small subset of T lymphocytes, the antigen-specific naïve T lymphocytes, are clonally selected and activated. Each individual antigen-specific naïve T cell can proliferate and expand into thousands of effector T lymphocytes. Following the clearance of antigens, most of effector T lymphocytes die, whereas a minor portion of the effector T lymphocytes transition to memory T cells, which are prepared to react rapidly to the same antigen in the future [1, 2]. However, during chronic viral infection or in the cancer microenvironment, T lymphocytes are exposed to persistent antigens, and become exhausted [3]. Exhausting T lymphocytes gradually lose cytokine expression, and express multiple inhibitory receptors including PD-1, TIM-3, TIGIT, and LAG-3 [4]. As a result, exhausted T lymphocytes have lost their ability to control infections or tumor growth [5].

The molecular and cellular mechanisms involved in T cell exhaustion have been extensively studied in order to design therapeutic interventions to prevent T cell exhaustion. The

most commonly used model of CD8+ T cell exhaustion is LCMV-clone 13 infection. Chen Z et al performed single cell RNA-seq analysis of LCMV-specific P14 cells on day 8 following LCMV-clone 13 infection, compared with LCMV-Armstrong infection [6]. Naïve P14 CD8+ T lymphocytes express TCF1 (encoded by *Tcf7* gene) and Ly108 (encoded by *Slamf6* gene); LCMV-Armstrong specific effector P14 CD8+ T lymphocytes express abundant Granzyme B, but low levels of TCF1, TOX, or PD-1. By contrast, LCMV-Clone 13 infection induces the exhaustion state of P14 CD8+ T lymphocytes, which have lost TCF1, and instead express high amounts of TOX, PD-1 and low level of cytotoxic molecules. Philip et al studied T cell exhaustion against tumor antigen SV40 [7]. It is found that as early as on day 5 after CD8+ T cell transfer, SV40-specific CD8+ T lymphocytes in the liver have already started to express exhaustion markers PD-1 and Lag3, and could not produce cytokine IFN-γ or TNF-α.

Besides cytotoxic CD8+ T lymphocytes, helper CD4+ T lymphocytes have a critical role in adaptive immunity [8]. Particularly, emerging evidence indicates that CD4+ T lymphocytes have a crucial role in antitumor immunity. CD4+ helper T lymphocytes can aid CD8+ T lymphocytes to target tumors [9]. CD4+ T lymphocytes directly engage conventional type 1 dendritic cells (cDC1) via CD40 signaling and to license cDC1 to prime tumor antigen-specific CD8+ T lymphocytes [10]. In mice, tumor antigen-specific CD4+ T lymphocytes can acquire the cytolytic ability and eradicate the subcutaneous melanoma in lymphatic ablated recipient mice through an MHC-II-dependent manner [11-13]. In human bladder cancer, it is intratumoral cytotoxic CD4+ T lymphocytes, but not canonical CD8+ T lymphocytes, that mediate anticancer immunity [14].

Whether tumor-specific CD4+ T lymphocyte exhaustion exists in tumor microenvironment and whether checkpoint blockade can prevent effector CD4+ T cell from being exhausted have not been clearly established. Hence, in this study we have studied the function state transition of tumor antigen-specific CD4+ T lymphocytes after adoptively transferred into lymphopenic recipient mice bearing large subcutaneous melanoma and dissected the mechanism by which immune checkpoint blockade prevents the transition of CD4+ T lymphocytes to the exhaustion state.

Materials and methods

Mice

C57BL/6 (CD45.1), Rag1-/-, and Tyrp1B-wRAG-/- TRP-1-specific CD4+ TCR transgenic mice were obtained from the Jackson Laboratory (Bar Harbor, MA). Because RAG is a key enzyme involved in V(D)J recombination, RAG knockout mice contain no T cells, B cells, or NKT cells which all play important roles in anticancer immunity. TRP-1 TCR transgene is located on the Y chromosome. CD4+ T lymphocytes in Tyrp1B-wRAG-/- TRP-1 male mice (CD4+ Vβ14+) express a transgenic TCR that recognizes the melanoma differentiation antigen tyrosinase-related protein 1 (TRP-1). All mice used in this study were handled in accordance with guidelines of the Comparative Medicine Program at Houston Methodist Research Institute (HMRI).
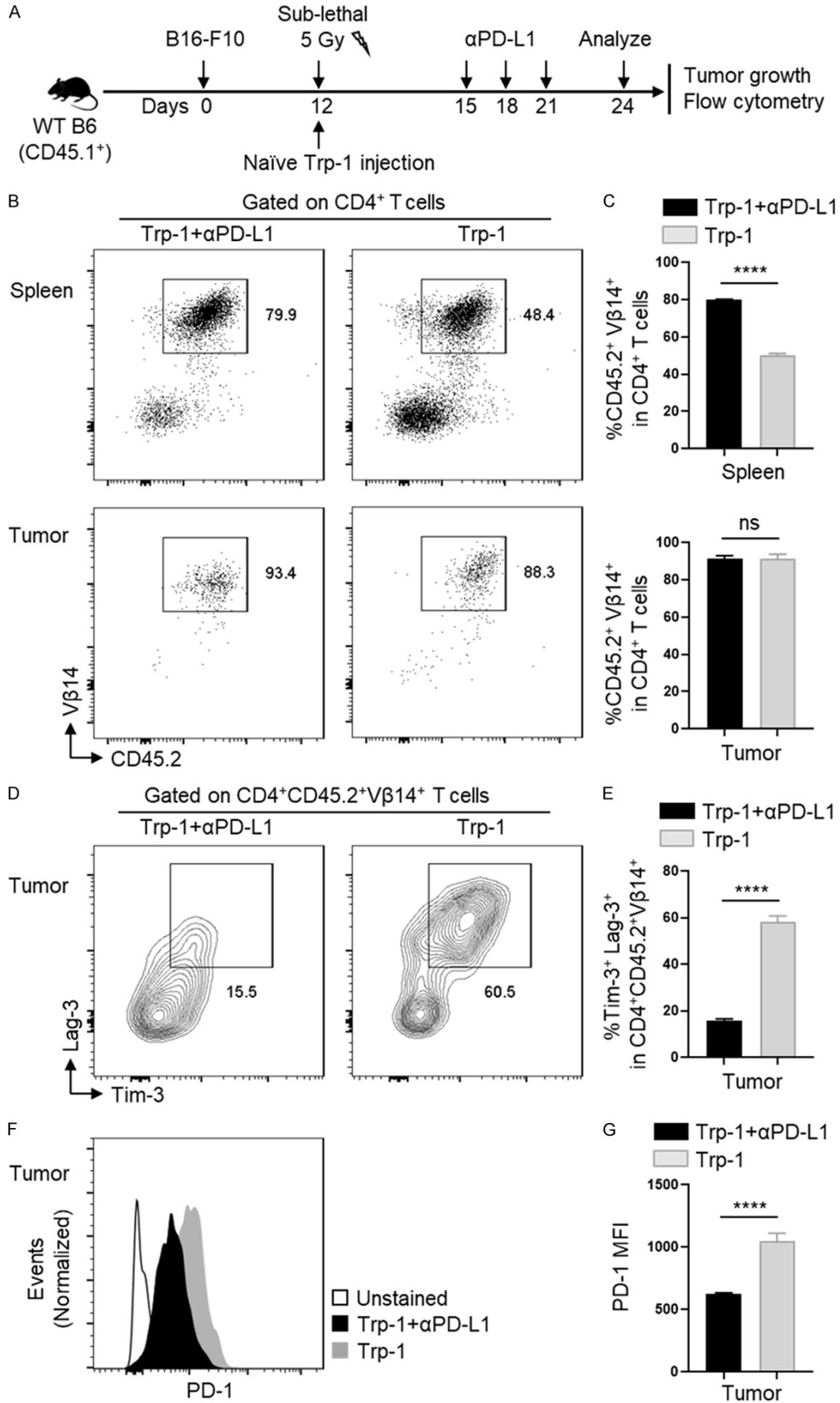
Tumor cell line and in vitro cell culture

The mouse B16F10 melanoma cells (American Type Culture Collection) were maintained in Dulbecco's Modified Eagle Medium (DMEM) (Thermo Fisher Scientific) containing 10% fetal bovine serum, 1% Penicillin/Streptomycin in 37°C incubator equilibrated with 5% CO_2.

Ectopic tumor implantation and tumor volume measurement

The right flank of C57BL/6 (CD45.1) or Rag1-/- mouse was shaved and subcutaneously (sc) injected with 0.5×10^6 B16F10 cells on day 0. Tumor volume was measured in two dimensions (length and width) using a vernier caliper every two days. Tumor volume was determined using the following formula: volume (cm^3) = $0.5 \times$ length $\times$ (width)^2. Mice were euthanized at the indicated time points, or when tumor volume reaches the endpoint (volume >2 cm^3, diameter >2 cm), or when mouse develops signs of discomfort (head tilt, weakness, or severely dehydrated), in accordance with recommendations approved by the 2000 Report of the American Veterinary Medical Association panel on euthanasia and the IACUC Committee at Houston Methodist Research Institute.

CD4⁺ T cell exhaustion

A. WT B6 (CD45.1⁺). Timeline: B16-F10 at Day 0; Sub-lethal 5 Gy and Naïve Trp-1 injection at Day 12; αPD-L1 at Days 15, 18, 21; Analyze at Day 24 → Tumor growth, Flow cytometry.

B. Gated on CD4⁺ T cells. Trp-1+αPD-L1 vs Trp-1. Spleen: 79.9, 48.4. Tumor: 93.4, 88.3. Axes: Vβ14 vs CD45.2.

C. %CD45.2⁺ Vβ14⁺ in CD4⁺ T cells. Spleen ****, Tumor ns.

D. Gated on CD4⁺CD45.2⁺Vβ14⁺ T cells. Tumor. Trp-1+αPD-L1: 15.5; Trp-1: 60.5. Axes: Lag-3 vs Tim-3.

E. %Tim-3⁺ Lag-3⁺ in CD4⁺CD45.2⁺Vβ14⁺ Tumor ****.

F. Tumor. Events (Normalized) vs PD-1. Unstained, Trp-1+αPD-L1, Trp-1.

G. PD-1 MFI. Tumor ****.

Figure 1. Anticancer activity of adoptively transferred Trp-1 CD4+ T lymphocytes in mice bearing subcutaneous melanoma and efficacy of co-treatment with immune checkpoint blockade. A. Schematic diagram showing the treatment regimen and the timeline for mice bearing melanoma. On day 24 post-tumor inoculation, the adoptively transferred Trp-1 CD4+ T lymphocytes isolated from irradiated WT B6 (CD45.1+) recipient mice were examined. All plots and histograms of flow cytometric analysis were gated on adoptively transferred CD4+ T lymphocytes among living splenocytes and TILs. B and C. Proportions of Trp-1 CD4+ T lymphocytes (CD45.2+Vβ14+) among gated total CD4+ T lymphocytes isolated from spleens and tumors on day 24. D and E. Representative flow and bar graphs of Tim-3 and Lag-3 expression on tumor infiltrating Trp-1 CD4+ T lymphocytes of each treatment group. F and G. PD-1 expression in tumor infiltrating Trp-1 CD4+ T lymphocytes of each treatment group. Experiments were repeated three times independently and data are presented as mean ± SD (n=4) from one representative experiment. Not significant = ns: P value >0.05; *: P<0.05; **: P<0.01; ***: P<0.001; ****: P<0.0001. Unpaired 2-tailed Student's t test.
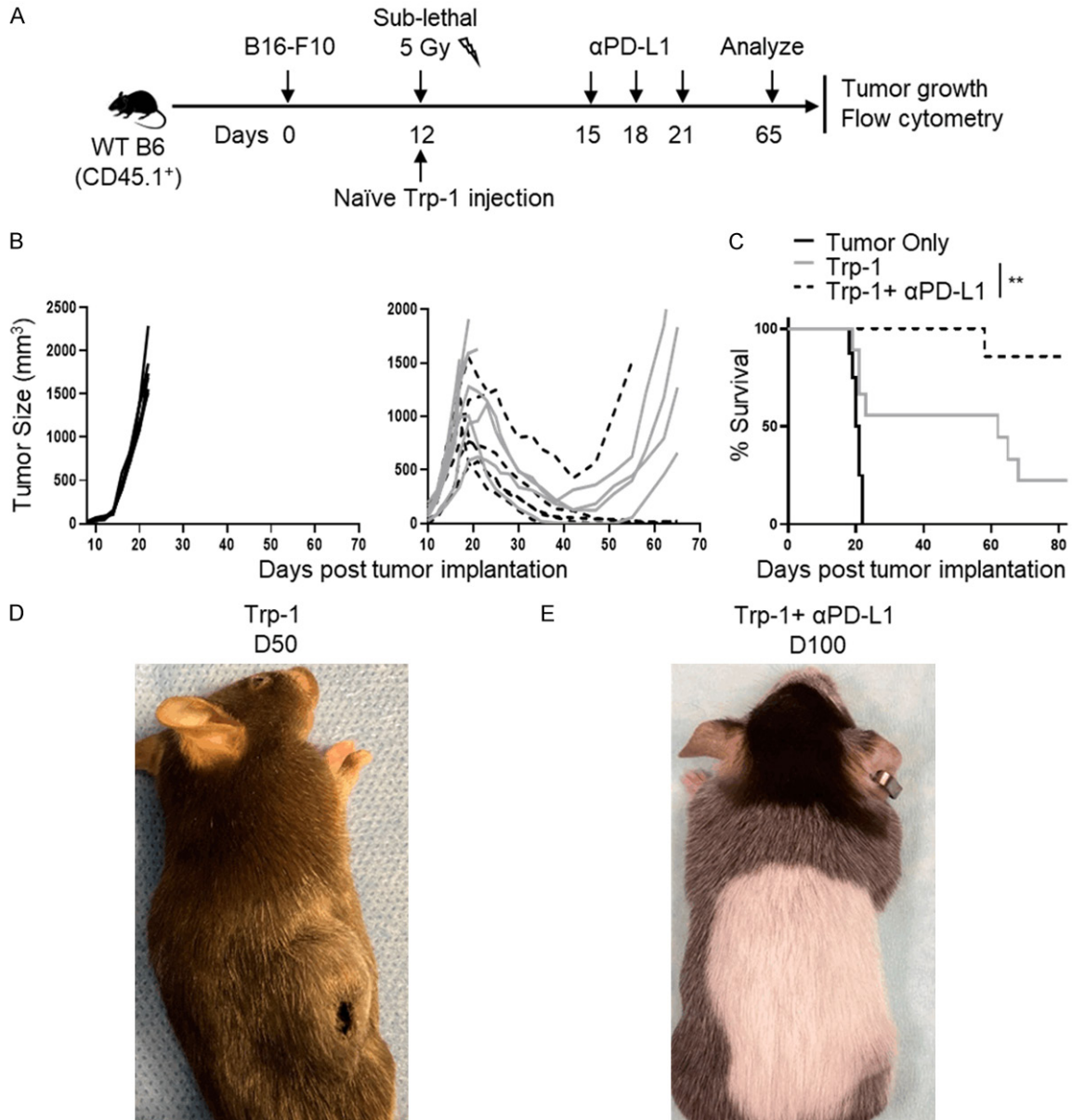

Figure 2. Adoptively transferred CD4+ T lymphocytes induced temporary regression of large established tumors, and prevention of tumor relapse by immune checkpoint blockade. (A) Schematic diagram showing the treatment regimen and the timeline for mice bearing large melanoma. WT B6 (CD45.1+) mice bearing B16F10 mouse melanoma (tumor diameter ~0.8 cm) received sublethal 5 Gy whole body irradiation and iv injected with tumor-specific Trp-1 CD4+ T lymphocytes. On day 15, 18 and 21, αPD-L1 or PBS control was administered for three times. Tumor size was measured with caliper every two days. (B) The growth curves of subcutaneous B16F10 melanoma in mice receiving

three different treatment regimens: no treatment, Trp-1 CD4$^+$ T cells/PBS, and Trp-1 CD4$^+$ T cells/αPD-L1. (C) Survival curves of mice receiving different treatment regimens based on the log-rank test. Data shown were combined from two independent experiments (n≥6 per group). **: *P*<0.01. The tumor pictures of representative recipient mice that received Trp-1 CD4$^+$ T cells/PBS on day 50 (D) and Trp-1 CD4$^+$ T cells/αPD-L1 on day 100 (E).

Adoptive transfer of antigen-specific Trp-1 CD4$^+$ T lymphocytes and immune checkpoint blockade

10 to 12 days after implantation, tumor diameter reached 0.8 to 1 cm, and mice received sub-lethal (5 Gy) whole body radiation. Adult male Tyrp1^{B-w}RAG$^{-/-}$ TRP-1 CD4$^+$ TCR transgenic mice (CD45.2) were euthanized, and spleen and lymph node cells were collected and filtered through a 70 μm cell strainer. Trp-1 CD4$^+$ T lymphocytes were purified with Dynabeads™ Mouse CD4 Kit (Thermo Fisher Scientific). Irradiated recipient mice bearing B16F10 melanoma tumors were grafted with 5 × 10^4 purified Trp-1 CD4$^+$ T lymphocytes through intravenous (iv) injection. After Trp-1 CD4$^+$ T lymphocyte graft, mice were administered with either PBS or anti-PD-L1 monoclonal antibody (10F9G2, Bio X Cell) by intraperitoneal (ip) injection for 3 times, on day 15, day 18 and day 21, at a dose of 10 μg/g of body weight.

Tumor digestion and single cell suspensions

Mice were euthanized at indicated time points. Tumors were excised, sliced into small pieces, enzymatically digested with collagenase I (SCR103 Sigma-Aldrich) and DNase I (AMPD1, Sigma-Aldrich) in RPMI1640 (R6504, Sigma-Aldrich) medium at 37°C for 30 minutes, and mashed through a 70 μm cell strainer to disperse cells. Tumor infiltrating lymphocytes (TILs) were purified using Ficoll density gradient (GE Healthcare). Cells between the interfaces of the liquid layers were harvested and washed with PBS twice prior to cell staining. Mouse splenocytes were filtered through a 70 μm cell strainer, washed with PBS twice, and ACK lysing buffer (Gibco) was added to selectively deplete red blood cells.

Flow cytometry analysis of cell surface markers and intracellular factors

The TILs and splenocytes isolated from the mice were stained with Zombie Aqua dye (Biolegend) for 15 minutes at room temperature to identify live cells. For cell surface marker staining, antibodies that recognize the following murine markers were purchased from

Thermo Fisher Scientific, including CD45.1 (A20), CD45.2 (104), CD4 (RFT-4g), CD62L (MEL-14), CD160 (CNX46-3), CD44 (IM7), CXCR6 (DANID2), Slamf6 (13G3-19D), Tim-3 (RMT3-23), Lag-3 (C9B7W), PD-1 (J43). Anti-mouse Vβ14 antibody (MR12-3) was purchased from BD Biosciences.

Intracellular transcription factors were stained with Foxp3/Transcription Factor Staining Buffer Set (eBioscience) for flow cytometry analysis. Mouse-specific Ki67 (SolA15) was purchased from Thermo Fisher Scientific and Anti-TCF1 rabbit mAb (C63D9) was purchased from Cell Signal Technology. Cytokines were stained with Fixation/Permeabilization Solution Kit with BD GolgiPlug (BD Biosciences). Lymphocytes were stimulated with 500 ng/ml ionomycin (Sigma-Aldrich), 50 ng/ml PMA (Sigma-Aldrich), and GolgiPlug (BD Biosciences) for 4 hrs in RPMI 1640 medium before cytokine staining. Antibodies against mouse IFN-γ (XMG1.2) and TNF-α (MP6-XT22) were obtained from Thermo Fisher Scientific.

TILs and splenocytes stained with different antibodies were analyzed on BD LSR II or BD LSRFortessa Flow Cytometer (BD Biosciences) at the HMRI Flow Cytometry Core. The data were analyzed manually with FlowJo software (version10, Tree Star).
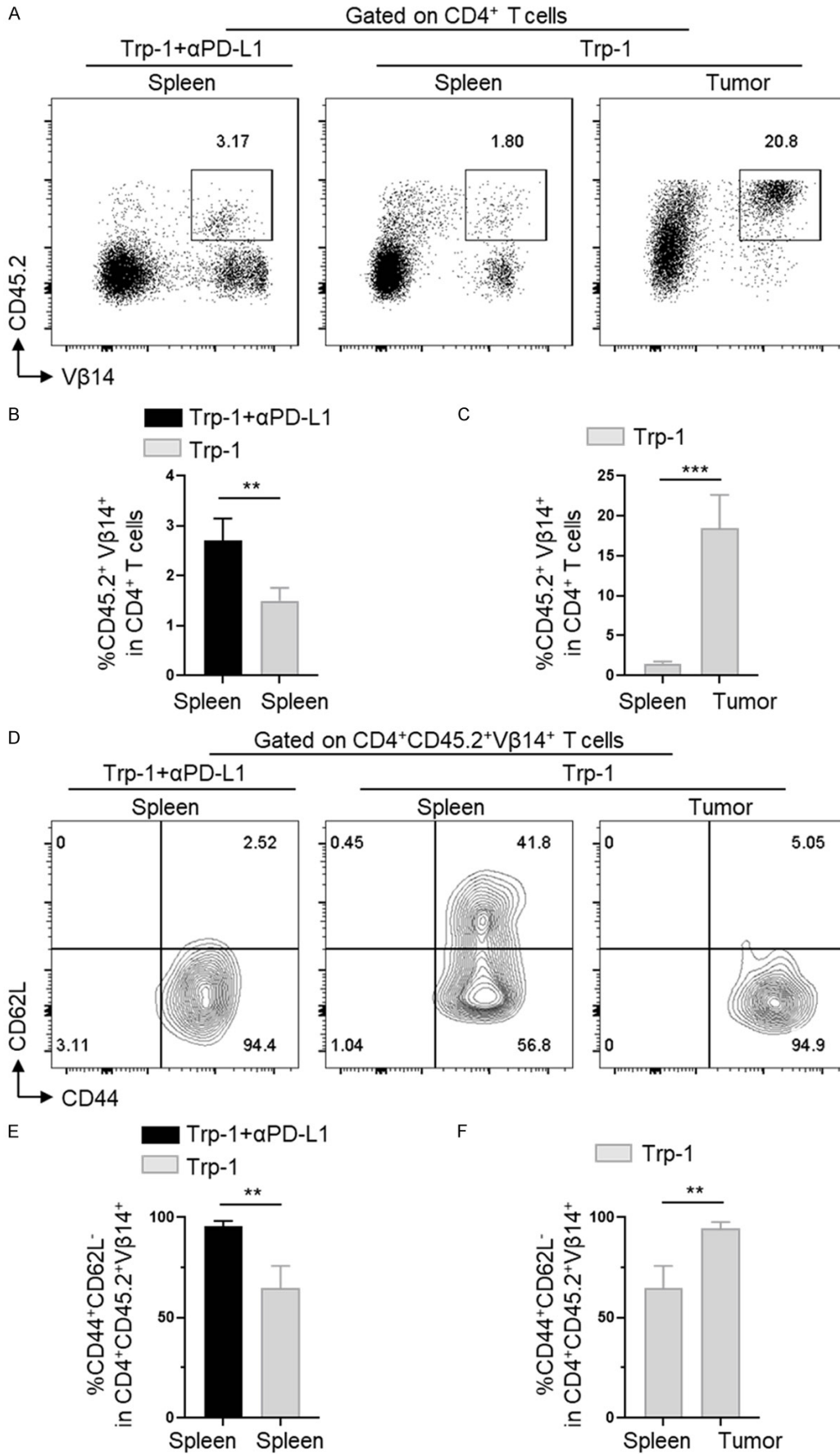
Statistical analysis

Mice were randomly assigned to control group and treatment group. The data were processed using GraphPad Prism8 and presented as mean ± SD. The means of the two sample groups were compared by using an unpaired 2-tailed Student's *t* test. The *p*-value of animal survival was determined by the log-rank test. A *p*-value less than 0.05 is regarded as statistically significant.

Results

Tumor-infiltrating TRP-1-specific CD4$^+$ T lymphocytes displayed an exhaustion phenotype, which was prevented by immune checkpoint blockade

We were interested in understanding how tumor-specific Trp-1 CD4$^+$ T lymphocytes

CD4+ T cell exhaustion

A   Gated on CD4+ T cells

Trp-1+αPD-L1 | Trp-1

Spleen | Spleen | Tumor

3.17 | 1.80 | 20.8

CD45.2

Vβ14

B

Trp-1+αPD-L1
Trp-1

%CD45.2+ Vβ14+ in CD4+ T cells

Spleen Spleen

**

C

Trp-1

%CD45.2+ Vβ14+ in CD4+ T cells

Spleen Tumor

***

D   Gated on CD4+CD45.2+Vβ14+ T cells

Trp-1+αPD-L1 | Trp-1

Spleen | Spleen | Tumor

0 | 2.52 | 0.45 | 41.8 | 0 | 5.05
3.11 | 94.4 | 1.04 | 56.8 | 0 | 94.9

CD62L

CD44

E

Trp-1+αPD-L1
Trp-1

%CD44+CD62L− in CD4+CD45.2+Vβ14+

Spleen Spleen

**

F

Trp-1

%CD44+CD62L− in CD4+CD45.2+Vβ14+

Spleen Tumor

**

Figure 3. Checkpoint blockade induced proliferative response and terminal effector phenotype in Trp-1 CD4$^+$ T lymphocytes. WT B6 (CD45.1$^+$) mice bearing B16F10 murine melanoma were adoptively transferred with 5 × 10^4 naïve Trp-1 CD4$^+$ T lymphocytes. On day 65 post-tumor inoculation, Trp-1 CD4$^+$ T lymphocytes were isolated from spleens and tumors and analyzed by flow cytometry. All plots and histograms were gated on transferred Trp-1 CD4$^+$ T lymphocytes among living splenocytes and TILs. A-C. The proportions of Trp-1 CD4$^+$ T lymphocytes (CD45.2$^+$Vβ14$^+$) among gated total CD4$^+$ T lymphocytes in spleens (Trp-1 CD4$^+$ T cells/αPD-L1) or in spleens and tumors (Trp-1 CD4$^+$ T cells/ PBS). D-F. The percentage of CD62L$^-$CD44$^+$ terminal effector T lymphocytes among the transferred Trp-1 CD4$^+$ T lymphocytes. Data are presented as mean ± SD (n=4). **: P<0.01, ***: *P*<0.001. Unpaired 2-tailed Student's *t* test.

respond when they encounter an excessive amount of tumor antigens in mice. WT B6 (CD45.1$^+$) mice were subcutaneously inoculated with 5 × 10^5 B16F10 murine melanoma cells on day 0. Twelve days after implantation, when tumor diameter reached to 0.8-1 cm, mice were treated with sublethal 5-Gy total body irradiation to remove homeostatic cytokine sinks [15]. Six hours later on the same day, 5 × 10^4 freshly isolated naïve Trp-1 cells from 8-week-old male Trp-1 CD4$^+$ TCR transgenic mice were intravenously injected into the irradiated mice. In addition, to test the effect of immune checkpoint blockade on TRP-1 CD4$^+$ T lymphocytes, mice were randomly divided into two groups and each group received αPD-L1 antibody or PBS via ip injection (**Figure 1A**). On day 24, mice were euthanized, tumors were excised, and tumor infiltrating lymphocytes (TILs) were purified.

The gating strategy for detecting the Trp-1 CD4$^+$ T lymphocytes is shown in Supplementary Figure 1A. Flow cytometry analyses indicate that, in comparison with PBS treatment group, mice treated with αPD-L1 possessed a significantly higher percentage of Trp-1 CD4$^+$ T lymphocytes in the spleen, 79.9% vs 48.4% (**Figure 1B**, **1C**). There was no difference in the percentage of tumor infiltrating Trp-1 CD4$^+$ T lymphocytes between αPD-L1 and PBS treatment groups (**Figure 1B**, **1C**). In comparison with cells purified from spleen, tumor infiltrating Trp-1 CD4$^+$ T lymphocytes lost Slamf6 expression and expressed high level of CXCR6, with or without αPD-L1 treatment (Supplementary Figure 1B). Moreover, there was a higher percentage of CD62L$^-$CD44$^+$ Trp-1 cells in spleens in mice treated with Trp-1 CD4$^+$ T lymphocytes/αPD-L1 compared with mice treated with the regimen of Trp-1 CD4$^+$ T cells/ PBS (Supplementary Figure 1C). Tumor infiltrating Trp-1 CD4$^+$ T lymphocytes lost the expression of CD62L, and instead expressed CD44, and became terminal-effector like T lymphocytes (data not shown). Meanwhile,

αPD-L1 treatment prevented the expression of exhaustion markers Tim-3 and Lag-3 in tumor infiltrating Trp-1 CD4$^+$ T lymphocytes (**Figure 1D**, **1E**). Additionally, αPD-L1 treatment decreased the PD-1 expression on Trp-1 CD4$^+$ T lymphocytes compared with PBS treatment (**Figure 1F**, **1G**). Hence, tumor-specific Trp-1 CD4$^+$ T lymphocytes indeed displayed the exhaustion phenotype after infiltration into tumors, which was alleviated by αPD-L1 immune checkpoint blockade.

Antitumor efficacy of adoptively transferred Trp-1 CD4$^+$ T lymphocytes on established melanoma in lymphopenic recipient mice

In a parallel experiment, the mice that were treated with Trp-1 CD4$^+$ T lymphocytes and αPD-L1 or PBS, were monitored for tumor growth and animal survival. Some mice were sacrificed on day 65 for flow cytometric analysis (**Figure 2A**). For the melanoma-bearing mice that did not receive any treatment, their tumor diameters reached 2 cm within 3 weeks (**Figure 2B**, left panel), and mice were euthanized. For mice that received Trp-1 CD4$^+$ T lymphocytes and αPD-L1 antibody or PBS, their tumors were rejected by day 30 to 40 (**Figure 2B**, right panel). However, in the Trp-1 CD4$^+$ T cells/PBS treatment group, their tumors regrew after a temporary regression (**Figure 2C**). Conversely, in the Trp-1 CD4$^+$ T cells/αPD-L1 treatment group, only one mouse had tumor relapse (**Figure 2B**, right panel, and **2C**). The difference in survival between these two groups is statistically significant. **Figure 2D** shows a recurrent tumor in a representative mouse administered with Trp-1 CD4$^+$ T cells/ PBS on day 50 post-tumor cell inoculation. **Figure 2E** shows complete tumor regression and significant vitiligo in a representative mouse administered with Trp-1 CD4$^+$ T cells/ αPD-L1 on day 100 post-tumor cell inoculation. Most of these mice that received Trp-1 CD4 T cells/αPD-L1 did not have tumor recurrence, and actually became autoimmune vitili-

CD4$^+$ T cell exhaustion

A

B

C

D

E

F
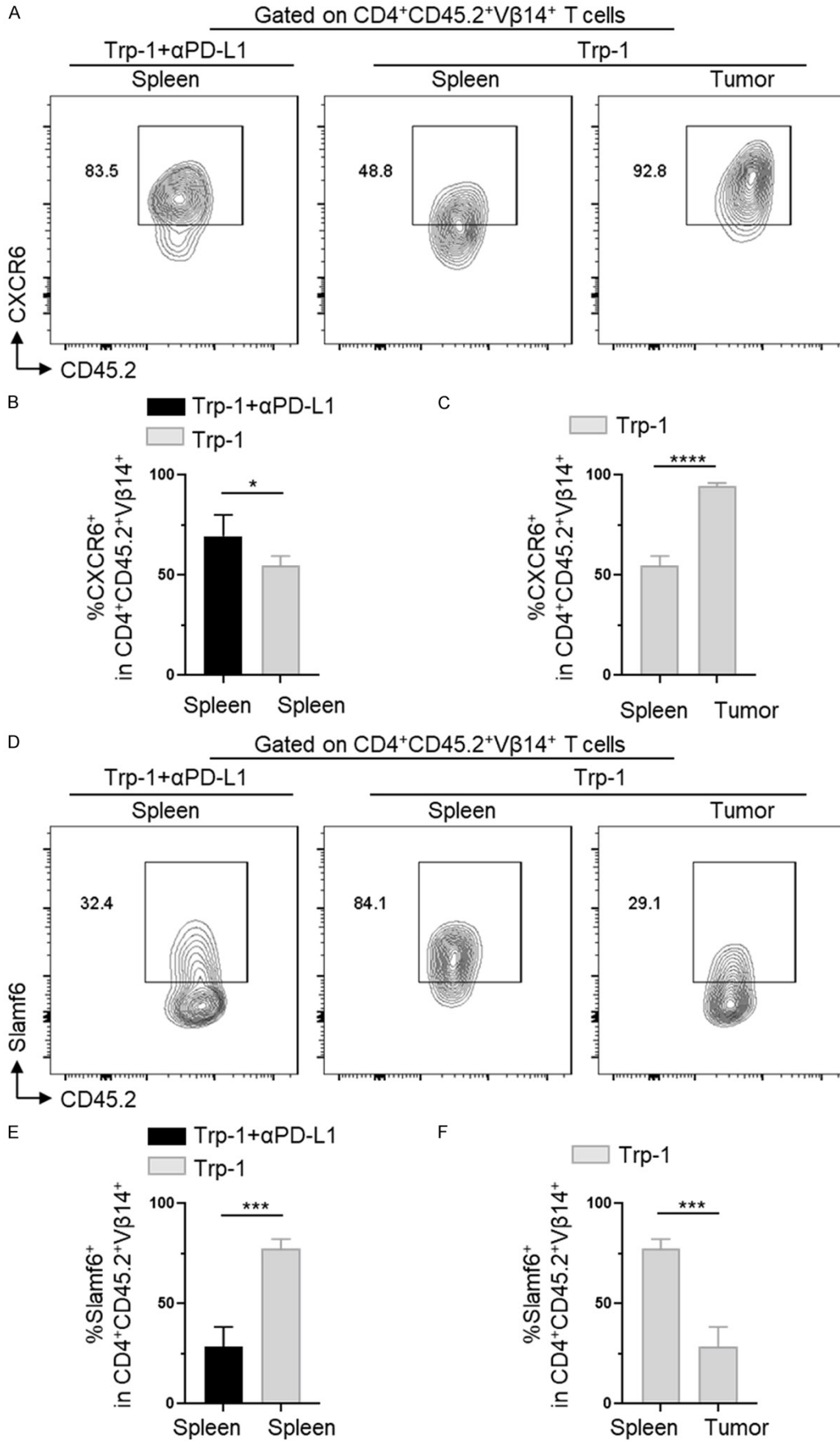
Figure 4. Checkpoint blockade prevented tumor relapse and altered the expression of CXCR6 and Slamf6 in Trp-1 CD4+ T lymphocytes. WT B6 (CD45.1+) mice bearing B16F10 mouse melanoma were adoptively transferred with 5 × 10^4 naïve Trp-1 cells. On day 65 post tumor inoculation, adoptively transferred Trp-1 CD4+ T lymphocytes were isolated from spleens and tumors and analyzed by flow cytometry. All plots and histograms of flow cytometric analysis were gated on adoptively transferred CD4+ T lymphocytes among living splenocytes and TILs. A-C. The percentage of CXCR6+ effector T lymphocytes among the transferred CD45.2+Vβ14+ Trp-1 cells in spleens (Trp-1 CD4+ T cells/αPD-L1) or in spleens and tumors (Trp-1 CD4+ T cells/PBS). D-F. Representative contour plots and bar graphs display the percentage of Slamf6+ T lymphocytes among the transferred CD45.2+Vβ14+ Trp-1 cells in spleens only (Trp-1 CD4+ T cell/αPD-L1) or spleens and tumors (Trp-1 CD4+ T cells/PBS). Data are presented as mean ± SD (n=4). *: $P<0.05$, ***: $P<0.001$, ****: $P<0.0001$. Unpaired 2-tailed Student's t test.

go, indicating the persistent in vivo activity of Trp-1 CD4+ T lymphocytes in the presence of αPD-L1. Our findings indicate that adoptive transfer of Trp-1 CD4+ T lymphocytes alone into sub-lethally irradiated lymphopenic recipient mice can cause regression of large established melanoma tumors; however tumor relapse is inevitable. Importantly, co-treatment with immune checkpoint αPD-L1 antibody can achieve complete tumor regression without recurrence.

Checkpoint blockade induced proliferative response of Trp-1 CD4+ T lymphocytes and their differentiation into effector T cell state

To further investigate the antitumor ability of Trp-1 CD4+ T lymphocytes, we examined the adoptively transferred Trp-1 CD4+ T lymphocytes in spleens and tumors from mice sacrificed on day 65 (**Figure 2A**). At this time point, tumors in mice administered with Trp-1 CD4+ T cells/αPD-L1 completely regressed. Therefore, we only analyzed the tumors from mice administered with Trp-1 CD4+ T cells/PBS. The results show that in peripheral lymphoid organs, the Trp-1 CD4+ T cells/αPD-L1-treated animals had a higher percentage of Trp-1 CD4+ T lymphocytes than Trp-1 CD4+ T cells/PBS treatment group (**Figure 3A**, **3B**). The percentage of Trp-1 CD4+ T lymphocytes in tumors was significantly higher than in peripheral lymphoid organs, indicating that antigen-specific Trp-1 CD4+ T lymphocytes were specifically recruited into tumors to exert tumor-killing function (**Figure 3A**, **3C**). In mice administered with Trp-1 CD4+ T cells/αPD-L1 combination regimen, Trp-1 CD4+ T lymphocytes had a higher capability of developing into CD62L-CD44+ T lymphocytes in the spleens (**Figure 3D**, **3E**), whereas the Trp-1 CD4+ T lymphocytes in the recurrence group displayed more CD62L+ CD44+ central memory-like phenotype in the spleens (**Figure 3D**). In contrast, the tumor infil-

trating Trp-1 CD4+ T lymphocytes in the tumor recurrence group lost CD62L expression, but expressed high level of CD44 (**Figure 3D**, **3F**).

In addition, we further analyzed the expression levels of Slamf6 and CXCR6 in Trp-1 CD4+ T lymphocytes. In comparison with PBS treatment group, Trp-1 CD4+ T lymphocytes from animals administered with αPD-L1 expressed higher level of CXCR6 in peripheral lymphoid organs (**Figure 4A**, **4B**). In the PBS treatment group, the tumor infiltrating Trp-1 CD4+ T lymphocytes expressed higher levels of CXCR6 than those cells in peripheral lymphoid organs (**Figure 4A**, **4C**). Because CXCR6 expression correlates with lymphocyte migration, in support of the observation that Trp-1 CD4+ T lymphocytes from animals treated with αPD-L1 had a higher capacity to infiltrate into tumors. Slamf6 is reported as a negative regulator of CD8+ T lymphocyte function and deficiency of Slamf6 increases anticancer activity of cytotoxic CD8+ T lymphocytes [16]. Our data show that, in peripheral lymphoid organs, Slamf6 expression level on Trp-1 CD4+ T lymphocytes from animals treated with αPD-L1 was significantly lower than those cells from mice treated with PBS (**Figure 4D**, **4E**). Meanwhile, the expression level of Slamf6 on tumor infiltrating Trp-1 CD4+ T lymphocytes was lower than those cells in spleens (**Figure 4D**, **4F**).

Taken together, αPD-L1 checkpoint blockade improved antitumor immunity of Trp-1 CD4+ T lymphocytes through inducing proliferative response and their differentiation toward effector T cell state in peripheral lymphoid organs.

Co-treatment with checkpoint blockade prevented tumor relapse by blocking Trp-1 CD4+ T cell transition to exhaustion state

To further dissect the mechanisms of checkpoint blockade in augmenting the antitumor efficacy of CD4+ T lymphocytes, we analyzed
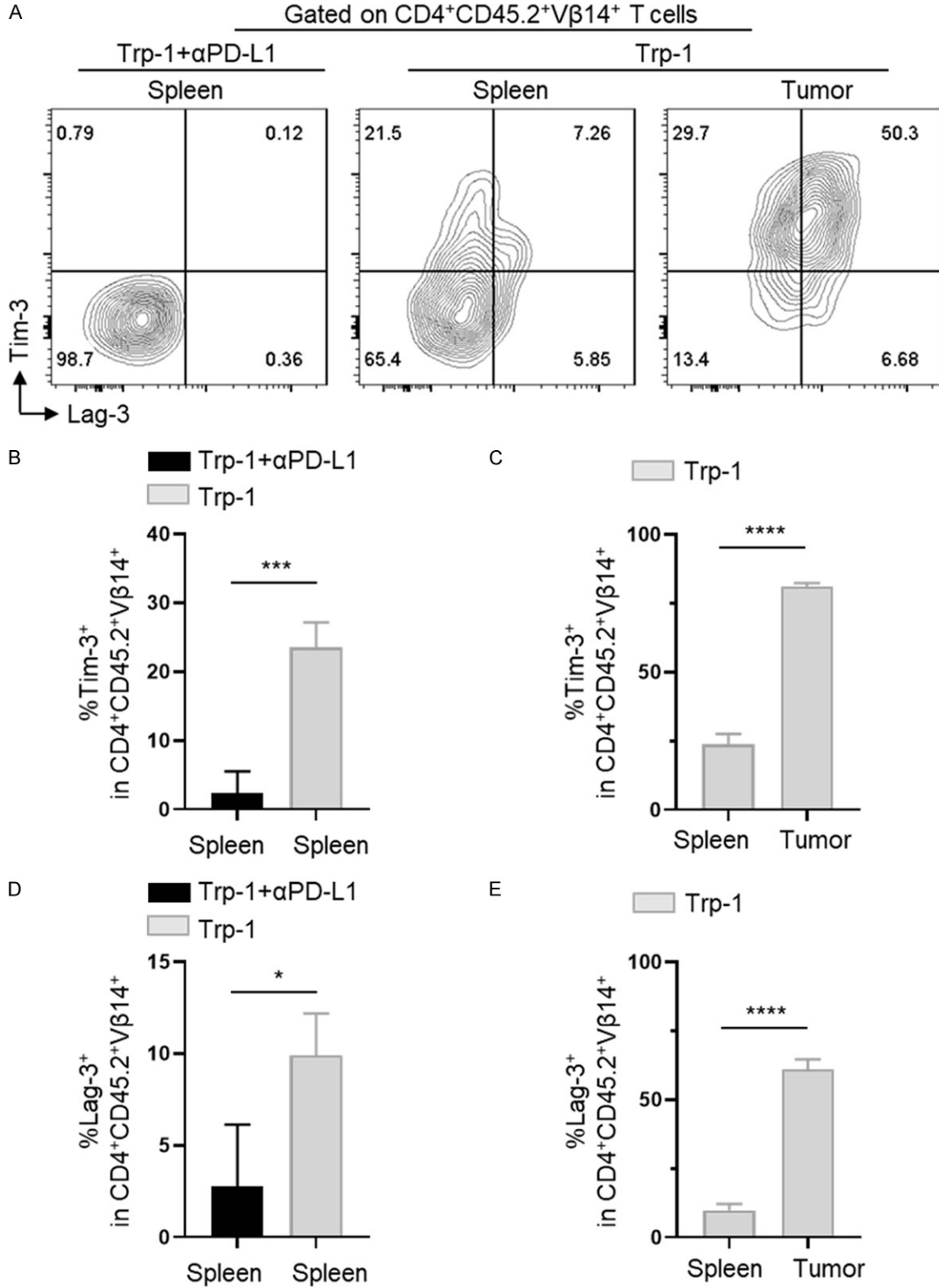
Figure 5. Checkpoint blockade inhibited the expression of exhaustion markers Tim-3 and Lag-3 in Trp-1 CD4+ T lymphocytes. WT B6 (CD45.1+) mice bearing B16F10 mouse melanoma were adoptively transferred with 5×10^4 naïve Trp-1 cells. Adoptively transferred Trp-1 cells isolated from spleens and tumors on day 65 post tumor inoculation and were analyzed by flow cytometry. All plots and histograms of flow cytometric analysis were gated on adoptively transferred CD4+ T lymphocytes among living splenocytes and TILs. A. The percentage of Tim-3+ and Lag-3+

exhausted T lymphocytes among the transferred CD45.2+Vβ14+ Trp-1 cells in spleens only (Trp-1 CD4+ T cells/αPD-L1) or in both spleens and tumors (Trp-1 CD4+ T cells/PBS). B and C. The percentage of Tim-3+ exhausted T lymphocytes among the transferred CD45.2+Vβ14+ Trp-1 cells in spleens only (Trp-1 CD4+ T cells/αPD-L1) or both spleens and tumors (Trp-1 CD4+ T cells/PBS). D and E. Bar graphs display the percentage of Lag-3+ exhausted T lymphocytes among the transferred CD45.2+Vβ14+ Trp-1 cells in spleens only (Trp-1 CD4+ T cells/αPD-L1) or both spleens and tumors (Trp-1 CD4+ T cells/PBS). Data are presented as mean ± SD (n=4). *: $P<0.05$, ***: $P<0.001$, ****: $P<0.0001$. Unpaired 2-tailed Student's *t* test.

the expression levels of exhaustion markers on the adoptively transferred Trp-1 CD4+ T lymphocytes on day 65 post-tumor implantation. Compared with PBS treatment group, Trp-1 CD4+ T lymphocytes from animals treated with αPD-L1 expressed low levels of Tim-3, Lag-3 (**Figure 5A**, **5B**, **5D**), PD-1 and CD160 (**Figure 6A**, **6B**, **6D**, **6E**) in peripheral lymphoid organs, indicating that αPD-L1 checkpoint blockade prevented the expression of inhibitory receptors on effector CD4+ T lymphocytes. By contrast, the expression levels of these exhaustion markers were significantly higher in tumor infiltrating Trp-1 CD4+ T lymphocytes likely caused by the immune suppression in the tumor microenvironment (**Figures 5A**, **5C**, **5E**, **6A**, **6C**, **6D** and **6F**). Hence, checkpoint blockade can prevent tumor recurrence by decreasing the expression of inhibitory receptors and avoiding CD4+ T cell exhaustion.

Checkpoint blockade did not affect the expression of Ki-67 while induce a progenitor-effector T cell phenotype in peripheral lymphoid organs

We next investigated the proliferative capacity of the adoptively transferred Trp-1 CD4+ T lymphocytes in WT B6 (CD45.1+) recipients on day 65 post-tumor inoculation. Shown in **Figure 7A** and **7B**, there was no difference in Ki-67 expression levels between the Trp-1 CD4+ T lymphocytes treated with αPD-L1 and PBS. In addition, the percentage of Ki-67 positive Trp-1 CD4+ T lymphocytes was similar in spleens and tumors among the PBS-treated recipients (**Figure 7A**, **7C**). The expression level of TCF-1, a key progenitor/naïve cell marker, was higher in Trp-1 CD4+ T lymphocytes isolated from the peripheral lymphoid organs of mice treated with αPD-L1 regimen (**Figure 7D**, **7E**). TCF-1+ CD8+ T lymphocytes are recognized as precursor-effector cells which are able to self-renew and produce more TCF-1- terminal effector T lymphocytes to increase anticancer immunity [17-19]. By contrast, tumor infiltrating Trp-1 CD4+ T lymphocytes all showed low

expression level of TCF-1 (not shown). Therefore, αPD-L1 checkpoint blockade did not affect the proliferative capacity of Trp-1 CD4+ T lymphocytes, and instead induced a precursor-effector T cell phenotype in peripheral lymphoid organs to expand antitumor immunity.

Checkpoint blockade increased cytokine production by Trp-1 CD4+ T lymphocytes

To further investigate the mechanisms of checkpoint blockade in promoting anticancer immunity of Trp-1 CD4+ T lymphocytes, we examined the production of anticancer cytokines by the adoptively transferred tumor-specific CD4+ T lymphocytes in WT B6 (CD45.1+) recipient mice on day 65 post-tumor implantation. Shown in **Figure 8A** and **8B**, Trp-1 CD4+ T lymphocytes isolated from spleens of animals treated with αPD-L1 expressed high amounts of IFN-γ and TNF-α, whereas Trp-1 CD4+ T lymphocytes isolated from spleens of mice treated with PBS barely expressed any of these cytotoxic molecules (**Figure 8A**, **8B**). Meanwhile, among PBS-treated recipient mice, the tumor infiltrating Trp-1 CD4+ T lymphocytes expressed higher levels of IFN-γ and TNF-α in comparison with Trp-1 CD4+ T lymphocytes in spleens (**Figure 8A**, **8C**). Therefore, checkpoint blockade helped Trp-1 CD4+ T lymphocytes produce more effector cytokines in peripheral lymphoid organs which prevented the recurrence of tumors.

Discussions

It is now well known that cytotoxic CD8+ T lymphocytes enter the state of exhaustion or dysfunction inside the immunosuppressive tumor microenvironment or encountering an excessive amount of tumor antigen. The immune checkpoint blockade therapies including anti-PD-1 and anti-PD-L1 monoclonal antibodies can mitigate CD8+ T cell exhaustion and rejuvenate anticancer immunity [17-20].

CD4$^+$ T cell exhaustion

A   Gated on CD4$^+$CD45.2$^+$Vβ14$^+$ T cells
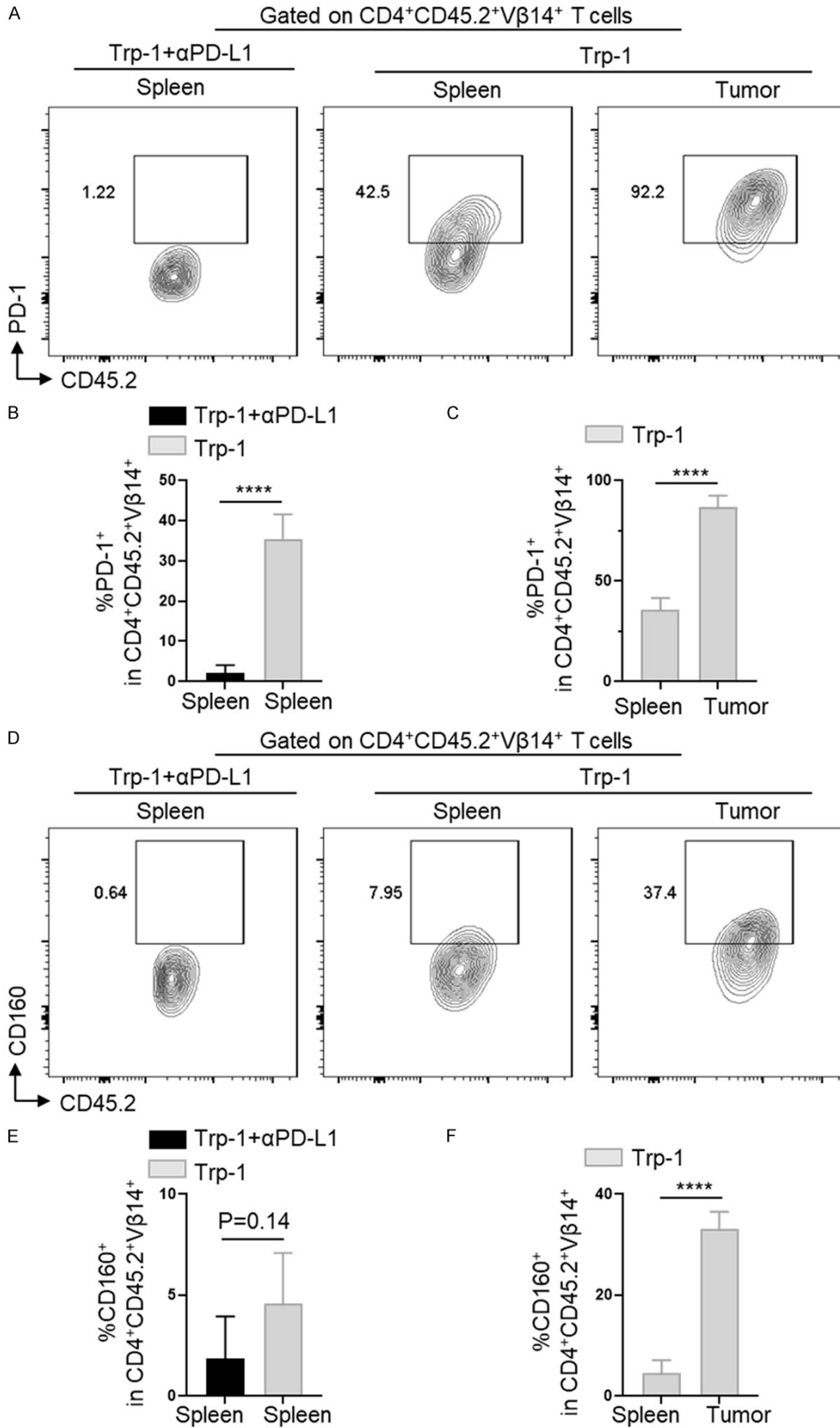
Figure 6. Checkpoint blockade inhibited the expression of exhaustion markers PD-1 and CD160 in Trp-1 CD4$^+$ T lymphocytes. WT B6 (CD45.1$^+$) mice bearing B16F10 murine melanoma were adoptively transferred with 5 × 10^4 naïve Trp-1 cells. Adoptively transferred Trp-1 cells isolated from spleens and tumors on day 65 post-tumor inoculation and analyzed by flow cytometry. All plots and histograms of flow cytometric analysis were gated on adoptively transferred CD4$^+$ T lymphocytes among living splenocytes and TILs. A-C. The percentage of PD-1$^+$ T lymphocytes among the transferred CD45.2$^+$Vβ14$^+$ Trp-1 cells in spleens only (Trp-1 CD4$^+$ T cells/αPD-L1) or both spleens and tumors (Trp-1 CD4$^+$ T cells/PBS). D-F. Representative contour plots and bar graphs display the percentage of CD160$^+$ T lymphocytes among the transferred CD45.2$^+$Vβ14$^+$ Trp-1 cells in spleens only (Trp-1 CD4$^+$ T cells/αPD-L1) or both spleens and tumors (Trp-1 CD4$^+$ T cells/PBS). Data are presented as mean ± SD (n=4). ****: *P*<0.0001. Unpaired 2-tailed Student's *t* test.

In this study, using a transgenic TCR Trp-1 CD4$^+$ T lymphocytes as an *in vivo* model, we have provided evidence that adoptively transferred tumor-specific Trp-1 CD4$^+$ T lymphocytes exhibited an exhaustion phenotype after infiltrating into solid tumors, resulting in tumor recurrence after a temporary regression. Similar to CD8$^+$ T lymphocytes, exhausted Trp-1 CD4$^+$ T lymphocytes also expressed typical inhibitory receptors including PD-1, Tim-3, Lag-3, and CD160. Importantly, the exhausted CD4$^+$ T lymphocytes also lost the expression of stemness marker TCF-1, in support of the critical role of TCF-1 in maintenance of precursor-effector subset of CD4$^+$ T lymphocytes. Tumor infiltrated Trp-1 CD4$^+$ T lymphocytes also lost the expression of CD62L and Slamf6 [16, 21], and instead expressed CD44 and CXCR6 [22].

However, this exhaustion can be prevented by co-treatment with anti-PD-L1 immune checkpoint blockade. When αPD-L1 antibody was co-administered with Trp-1 CD4$^+$ T lymphocytes to the recipient mice, the tumors were completely rejected and most of them did not relapse. Further flow cytometry analyses indicate that the Trp-1 CD4$^+$ T lymphocytes in peripheral lymphoid tissues showed a TCF1$^+$ stem-like phenotype in mice co-treated with αPD-L1. Moreover, we found that in lymphopenic B6.*Rag1*$^{-/-}$ recipients, which lack B and T lymphocytes, the tumors underwent complete regression and mice developed vitiligo (depigmentation) after a combination regimen with Trp-1 CD4$^+$ T lymphocytes and αPD-L1 (Supplementary Figure 2A, 2B), indicating the tumor rejection immunity was not contributed by endogenous B or T lymphocytes. Moreover, treatment with anti-PD-L1 antibody only did not have effect on the growth of B16F10 subcutaneous melanoma, or the functional states of endogenous CD4$^+$ and CD8$^+$ T lymphocytes (Supplementary Figures 3 and 4), indicating

that the antitumor effect of anti-PD-L1 antibody was mostly mediated by adoptively transferred tumor-specific Trp-1 CD4$^+$ T lymphocytes in this model.

In conclusion, after encountering an excessive amount of tumor antigen, tumor-specific CD4$^+$ T lymphocytes enter an exhaustion state, which clearly dampen their antitumor immunity, resulting in loss of tumor control. Fortunately, co-treatment with immune checkpoint blockade αPD-L1 can prevent the exhaustion and induce proliferation response of tumor-specific CD4$^+$ T lymphocytes. Our results suggest that the current commonly used immune checkpoint blockade therapies might achieve durable anticancer efficacy by rejuvenating tumor-specific CD4$^+$ T lymphocytes, in addition to conventional cytotoxic tumor antigen-specific CD8$^+$ T lymphocytes.

Acknowledgements

Disclosure of conflict of interest

None.

Address correspondence to: Bin He, Immunobiology & Transplant Science Center, Houston Methodist Research Institute, 6670 Bertner Avenue, R7-116, Houston, TX 77030, USA. Tel: 713-441-2049; Fax: 713-441-7439; E-mail: bhe@houston-methodist.org; Wenhao Chen, Immunobiology & Transplant Science Center, Houston Methodist Research Institute, 6670 Bertner Avenue, R7-216, Houston, TX 77030, USA. Tel: 713-441-2173; Fax:
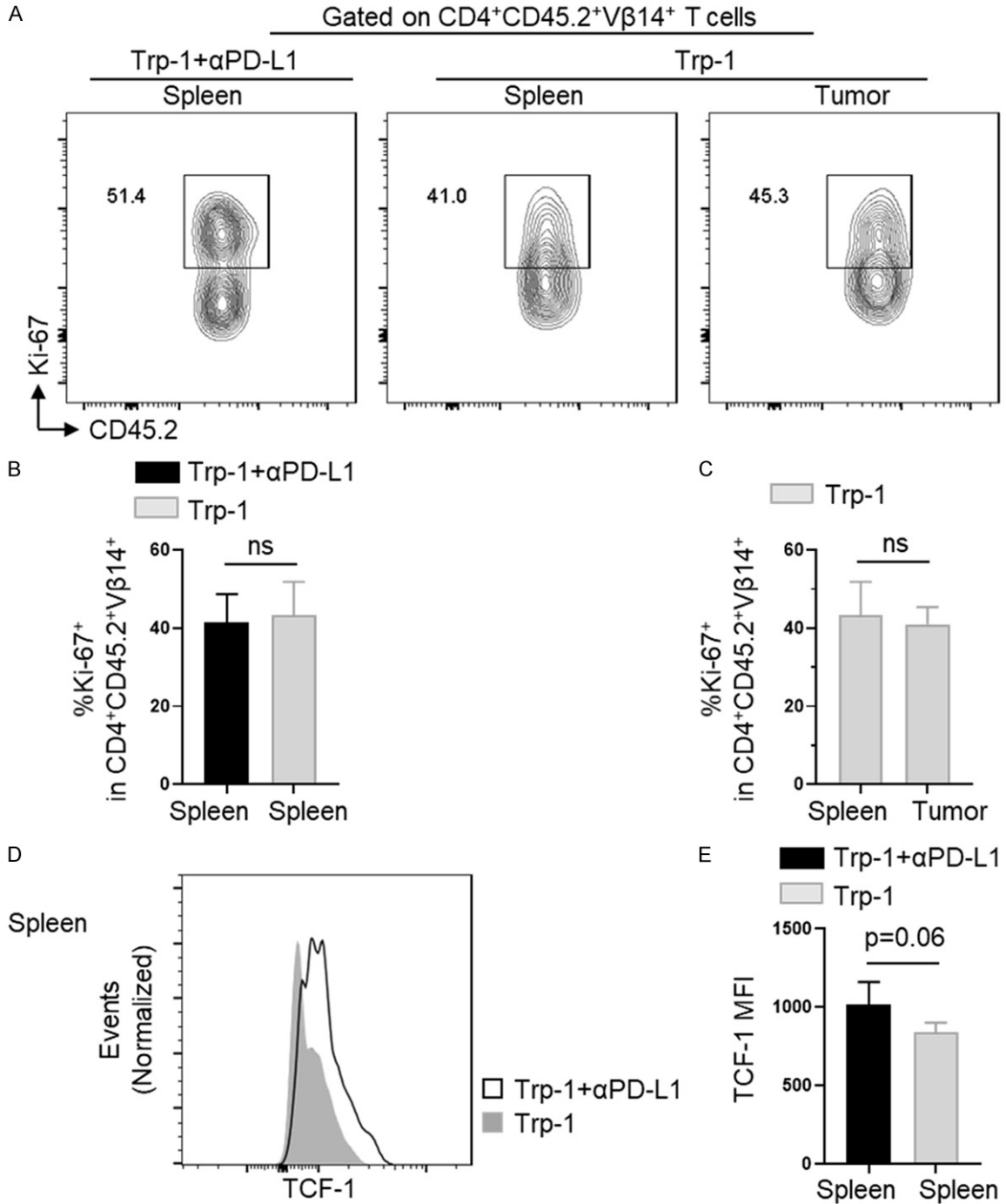
Figure 7. Checkpoint blockade did not affect the expression of Ki-67 while induced a progenitor-effector T cell phenotype in peripheral lymphoid organs. WT B6 (CD45.1+) mice bearing B16F10 mouse melanoma were adoptively transferred with 5×10^4 naïve Trp-1 CD4+ T lymphocytes. On day 65 post-tumor inoculation, adoptively transferred Trp-1 CD4+ T lymphocytes were isolated from spleens and tumors and were analyzed by flow cytometry. All plots and histograms of flow cytometric analysis were gated on adoptively transferred CD4+ T lymphocytes among living splenocytes and TILs. A-C. The percentage of Ki-67+ T lymphocytes among the transferred CD45.2+Vβ14+ Trp-1 cells in spleens only (Trp-1 CD4+ T cells/αPD-L1) or both spleens and tumors (Trp-1 CD4+ T cells/PBS). D and E. Overlay histogram and bar graphs display the mean fluoresce intensity of TCF-1 among the transferred CD45.2+Vβ14+ Trp-1 cells in spleens (Trp-1 CD4+ T cells/αPD-L1 group and Trp-1 CD4+ T cells/PBS group). Data are presented as mean ± SD (n=4). ns: *P*>0.05. Unpaired 2-tailed Student's *t* test.
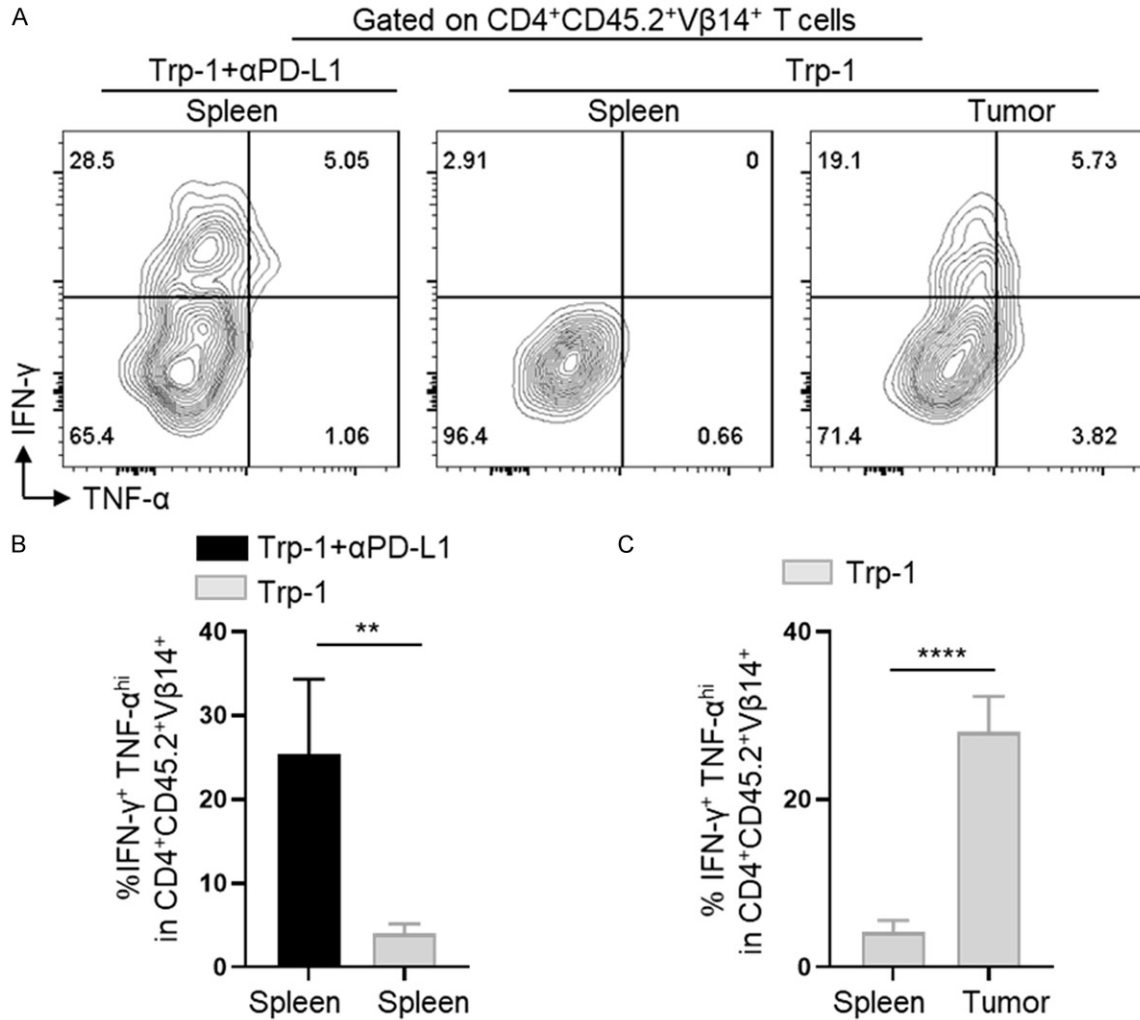
Figure 8. Checkpoint blockade increased Trp-1 CD4$^+$ T lymphocyte production of anticancer cytokines. WT B6 (CD45.1$^+$) mice bearing B16F10 mouse melanoma were adoptively transferred with 5 × 10^4 naïve Trp-1 CD4$^+$ T lymphocytes. On day 65 post-tumor inoculation, adoptively transferred Trp-1 cells were isolated from spleens and tumors and analyzed by flow cytometry. All plots and histograms of flow cytometric analysis were gated on adoptively transferred CD4$^+$ T cells among living splenocytes and TILs. A-C. The percentage of IFN-γ$^+$ TNF-α^{hi} T lymphocytes among the transferred CD45.2$^+$Vβ14$^+$ Trp-1 cells in spleens only (Trp-1 CD4$^+$ T cells/αPD-L1) or both spleens and tumors (Trp-1 CD4$^+$ T cells/PBS). Data are presented as mean ± SD (n=4). **: $P<0.01$, ****: $P<0.0001$. Unpaired 2-tailed Student's t test.

713-441-7439; E-mail: wchen@houstonmethodist.org

References

[1] Wu J, Zhang H, Shi X, Xiao X, Fan Y, Minze LJ, Wang J, Ghobrial RM, Xia J, Sciammas R, Li XC and Chen W. Ablation of transcription factor IRF4 promotes transplant acceptance by driving allogenic CD4(+) T cell dysfunction. Immunity 2017; 47: 1114-1128, e1116.

[2] Zhang H, Wu J, Zou D, Xiao X, Yan H, Li XC and Chen W. Ablation of interferon regulatory factor 4 in T cells induces "memory" of transplant tolerance that is irreversible by immune checkpoint blockade. Am J Transplant 2019; 19: 884-893.

[3] Blank CU, Haining WN, Held W, Hogan PG, Kallies A, Lugli E, Lynn RC, Philip M, Rao A, Restifo NP, Schietinger A, Schumacher TN, Schwartzberg PL, Sharpe AH, Speiser DE, Wherry EJ, Youngblood BA and Zehn D. Defining 'T cell exhaustion'. Nat Rev Immunol 2019; 19: 665-674.

[4] Sekine T, Perez-Potti A, Nguyen S, Gorin JB, Wu VH, Gostick E, Llewellyn-Lacey S, Hammer Q, Falck-Jones S, Vangeti S, Yu M, Smed-Sörensen A, Gaballa A, Uhlin M, Sandberg JK, Brander C,

Nowak P, Goepfert PA, Price DA, Betts MR and Buggert M. TOX is expressed by exhausted and polyfunctional human effector memory CD8(+) T cells. Sci Immunol 2020; 5: eaba7918.

[5] Hudson WH, Gensheimer J, Hashimoto M, Wieland A, Valanparambil RM, Li P, Lin JX, Konieczny BT, Im SJ, Freeman GJ, Leonard WJ, Kissick HT and Ahmed R. Proliferating transitory T cells with an effector-like transcriptional signature emerge from PD-1(+) stem-like CD8(+) T cells during chronic infection. Immunity 2019; 51: 1043-1058, e1044.

[6] Chen Z, Ji Z, Ngiow SF, Manne S, Cai Z, Huang AC, Johnson J, Staupe RP, Bengsch B, Xu C, Yu S, Kurachi M, Herati RS, Vella LA, Baxter AE, Wu JE, Khan O, Beltra JC, Giles JR, Stelekati E, McLane LM, Lau CW, Yang X, Berger SL, Vahedi G, Ji H and Wherry EJ. TCF-1-centered transcriptional network drives an effector versus exhausted CD8 T cell-fate decision. Immunity 2019; 51: 840-855, e845.

[7] Philip M, Fairchild L, Sun L, Horste EL, Camara S, Shakiba M, Scott AC, Viale A, Lauer P, Merghoub T, Hellmann MD, Wolchok JD, Leslie CS and Schietinger A. Chromatin states define tumor-specific T cell dysfunction and reprogramming. Nature 2017; 545: 452-456.

[8] Borst J, Ahrends T, Bąbała N, Melief CJM and Kastenmüller W. CD4(+) T cell help in cancer immunology and immunotherapy. Nat Rev Immunol 2018; 18: 635-647.

[9] Alspach E, Lussier DM, Miceli AP, Kizhvatov I, DuPage M, Luoma AM, Meng W, Lichti CF, Esaulova E, Vomund AN, Runci D, Ward JP, Gubin MM, Medrano RFV, Arthur CD, White JM, Sheehan KCF, Chen A, Wucherpfennig KW, Jacks T, Unanue ER, Artyomov MN and Schreiber RD. MHC-II neoantigens shape tumour immunity and response to immunotherapy. Nature 2019; 574: 696-701.

[10] Ferris ST, Durai V, Wu R, Theisen DJ, Ward JP, Bern MD, Davidson JT 4th, Bagadia P, Liu T, Briseño CG, Li L, Gillanders WE, Wu GF, Yokoyama WM, Murphy TL, Schreiber RD and Murphy KM. cDC1 prime and are licensed by CD4(+) T cells to induce anti-tumour immunity. Nature 2020; 584: 624-629.

[11] Muranski P, Boni A, Antony PA, Cassard L, Irvine KR, Kaiser A, Paulos CM, Palmer DC, Touloukian CE, Ptak K, Gattinoni L, Wrzesinski C, Hinrichs CS, Kerstann KW, Feigenbaum L, Chan CC and Restifo NP. Tumor-specific Th17-polarized cells eradicate large established melanoma. Blood 2008; 112: 362-373.

[12] Xie Y, Akpinarli A, Maris C, Hipkiss EL, Lane M, Kwon EK, Muranski P, Restifo NP and Antony PA. Naive tumor-specific CD4(+) T cells differ-

[13] Quezada SA, Simpson TR, Peggs KS, Merghoub T, Vider J, Fan X, Blasberg R, Yagita H, Muranski P, Antony PA, Restifo NP and Allison JP. Tumor-reactive CD4(+) T cells develop cytotoxic activity and eradicate large established melanoma after transfer into lymphopenic hosts. J Exp Med 2010; 207: 637-650.

[14] Oh DY, Kwek SS, Raju SS, Li T, McCarthy E, Chow E, Aran D, Ilano A, Pai CS, Rancan C, Allaire K, Burra A, Sun Y, Spitzer MH, Mangul S, Porten S, Meng MV, Friedlander TW, Ye CJ and Fong L. Intratumoral CD4(+) T cells mediate anti-tumor cytotoxicity in human bladder cancer. Cell 2020; 181: 1612-1625, e1613.

[15] Gattinoni L, Finkelstein SE, Klebanoff CA, Antony PA, Palmer DC, Spiess PJ, Hwang LN, Yu Z, Wrzesinski C, Heimann DM, Surh CD, Rosenberg SA and Restifo NP. Removal of homeostatic cytokine sinks by lymphodepletion enhances the efficacy of adoptively transferred tumor-specific CD8+ T cells. J Exp Med 2005; 202: 907-912.

[16] Hajaj E, Eisenberg G, Klein S, Frankenburg S, Merims S, Ben David I, Eisenhaure T, Henrickson SE, Villani AC, Hacohen N, Abudi N, Abramovich R, Cohen JE, Peretz T, Veillette A and Lotem M. SLAMF6 deficiency augments tumor killing and skews toward an effector phenotype revealing it as a novel T cell checkpoint. Elife 2020; 9: e52539.

[17] Kurtulus S, Madi A, Escobar G, Klapholz M, Nyman J, Christian E, Pawlak M, Dionne D, Xia J, Rozenblatt-Rosen O, Kuchroo VK, Regev A and Anderson AC. Checkpoint blockade immunotherapy induces dynamic changes in PD-1(-) CD8(+) tumor-infiltrating T cells. Immunity 2019; 50: 181-194, e186.

[18] Siddiqui I, Schaeuble K, Chennupati V, Fuertes Marraco SA, Calderon-Copete S, Pais Ferreira D, Carmona SJ, Scarpellino L, Gfeller D, Pradervand S, Luther SA, Speiser DE and Held W. Intratumoral Tcf1(+)PD-1(+)CD8(+) T cells with stem-like properties promote tumor control in response to vaccination and checkpoint blockade immunotherapy. Immunity 2019; 50: 195-211, e110.

[19] Chen Z, Ji Z, Ngiow SF, Manne S, Cai Z, Huang AC, Johnson J, Staupe RP, Bengsch B, Xu C, Yu S, Kurachi M, Herati RS, Vella LA, Baxter AE, Wu JE, Khan O, Beltra JC, Giles JR, Stelekati E, McLane LM, Lau CW, Yang X, Berger SL, Vahedi G, Ji H and Wherry EJ. TCF-1-centered transcriptional network drives an effector versus exhausted CD8 T cell-fate decision. Immunity 2019; 51: 840-855, e845.

[20] Yost KE, Satpathy AT, Wells DK, Qi Y, Wang C, Kageyama R, McNamara KL, Granja JM, Sarin KY, Brown RA, Gupta RK, Curtis C, Bucktrout SL, Davis MM, Chang ALS and Chang HY. Clonal replacement of tumor-specific T cells following PD-1 blockade. Nat Med 2019; 25: 1251-1259.

[21] LaFleur MW, Nguyen TH, Coxe MA, Miller BC, Yates KB, Gillis JE, Sen DR, Gaudiano EF, Al Abosy R, Freeman GJ, Haining WN and Sharpe AH. PTPN2 regulates the generation of exhausted CD8(+) T cell subpopulations and restrains tumor immunity. Nat Immunol 2019; 20: 1335-1347.

[22] Holz LE, Chua YC, de Menezes MN, Anderson RJ, Draper SL, Compton BJ, Chan STS, Mathew J, Li J, Kedzierski L, Wang Z, Beattie L, Enders MH, Ghilas S, May R, Steiner TM, Lange J, Fernandez-Ruiz D, Valencia-Hernandez AM, Osmond TL, Farrand KJ, Seneviratna R, Almeida CF, Tullett KM, Bertolino P, Bowen DG, Cozijnsen A, Mollard V, McFadden GI, Caminschi I, Lahoud MH, Kedzierska K, Turner SJ, Godfrey DI, Hermans IF, Painter GF and Heath WR. Glycolipid-peptide vaccination induces liver-resident memory CD8(+) T cells that protect against rodent malaria. Sci Immunol 2020; 5: eaaz8035.

CD4+ T cell exhaustion
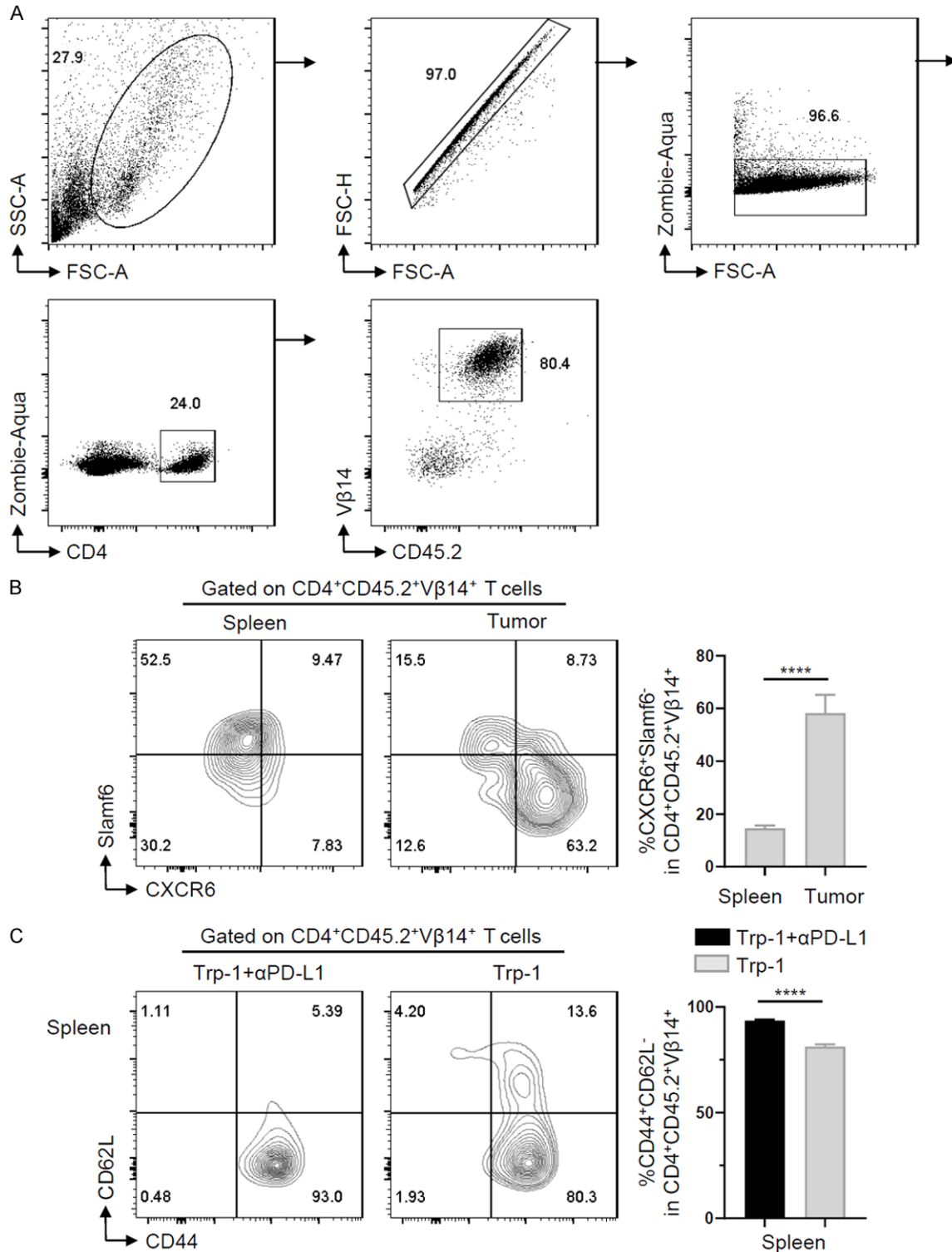
Supplementary Figure 1. Tumor-specific Trp-1 CD4+ T lymphocytes functional state transition. On day 24 post-tumor inoculation, the adoptively transferred Trp-1 CD4+ T lymphocytes in irradiated WT B6 (CD45.1+) mice were analyzed. A. Gating strategy for detecting the living CD4+CD45.2+Vβ14+ Trp-1 CD4+ T lymphocytes. B. The expression levels of Slamf6 and CXCR6 on Trp-1 CD4+ T lymphocytes in spleens and tumors. C. The percentage of CD62L-CD44+ effector memory/effector T lymphocytes among the transferred Trp-1 CD4+ T lymphocytes in spleens. Data are presented as mean ± SD (n=4). ****: P<0.0001. Unpaired 2-tailed Student's t test.
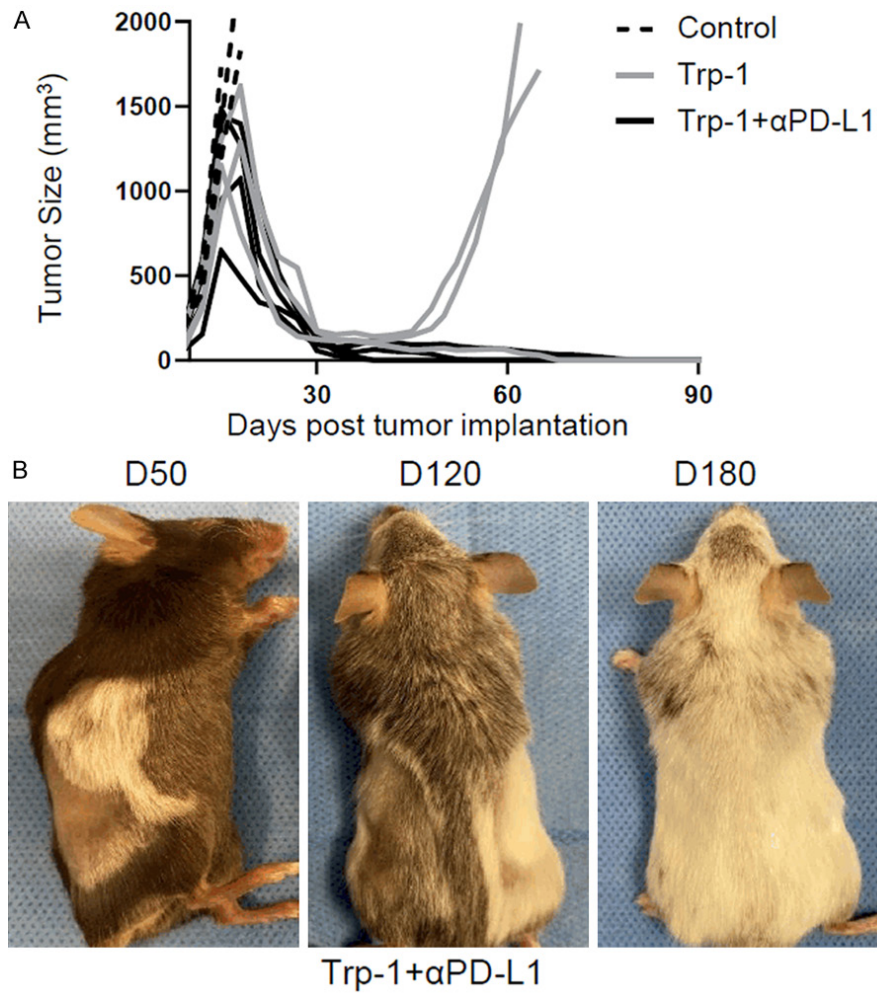
Supplementary Figure 2. Tumor-specific Trp-1 CD4+ T lymphocytes eradicated large established tumors in lymphopenic mice and induced autoimmune vitiligo in *Rag1-/-* mice. Combination treatment of 5 × 10^4 naïve Trp-1 CD4+ T lymphocytes with αPD-L1 or PBS were given to B6.*Rag1-/-* mice. Tumor volumes and depigmentation were monitored. A. Tumor volumes of non-treatment group (n=3), Trp-1 CD4+ T cells/PBS group (n=3), and Trp-1 CD4+ T cells/αPD-L1 group (n=4). B. The progressive development of vitiligo after combination treatment of Trp-1 CD4+ T lymphocytes and αPD-L1 antibody.

CD4+ T cell exhaustion
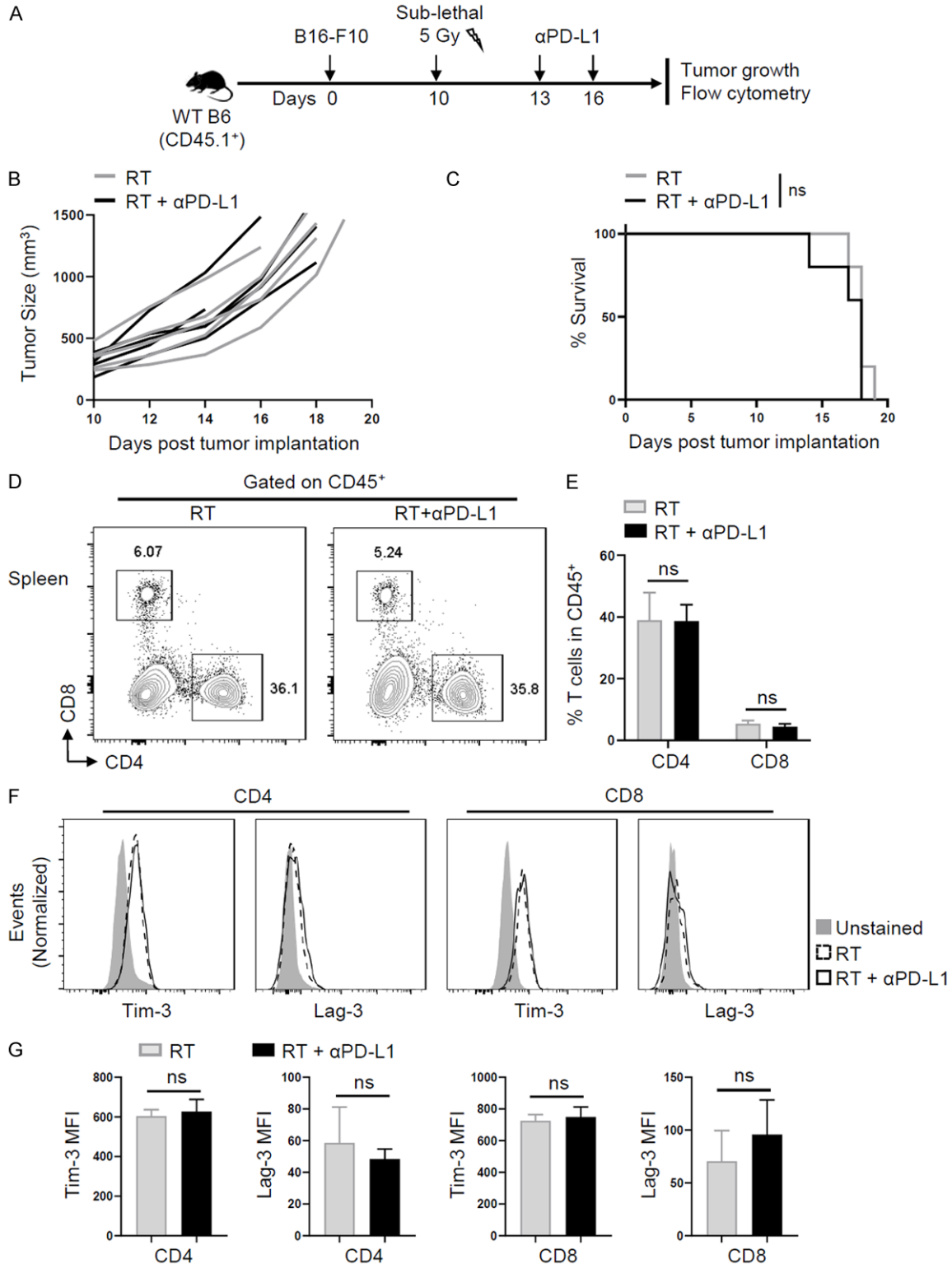
Supplementary Figure 3. Effect of αPD-L1 antibody alone on established melanoma. A. WT B6 (CD45.1+) mice bearing large B16F10 melanoma were treated with sub-lethal radiation therapy (RT, 5 Gy) and PD-L1 blockade at indicated time points. B. Tumor volumes of RT group (n=5) and RT/αPD-L1 group (n=5). C. Percent survival of B16F10 tumor-bearing mice in RT group (n=5) and RT/αPD-L1 group (n=5). D and E. Proportions of endogenous CD4+ and CD8+ T lymphocytes among gated CD45+ cells isolated from spleens on day 18. F and G. The expression levels of Tim-3 and Lag-3 on CD4+ and CD8+ T lymphocytes. Data are presented as mean ± SD (n=3). ns: *P*>0.05.
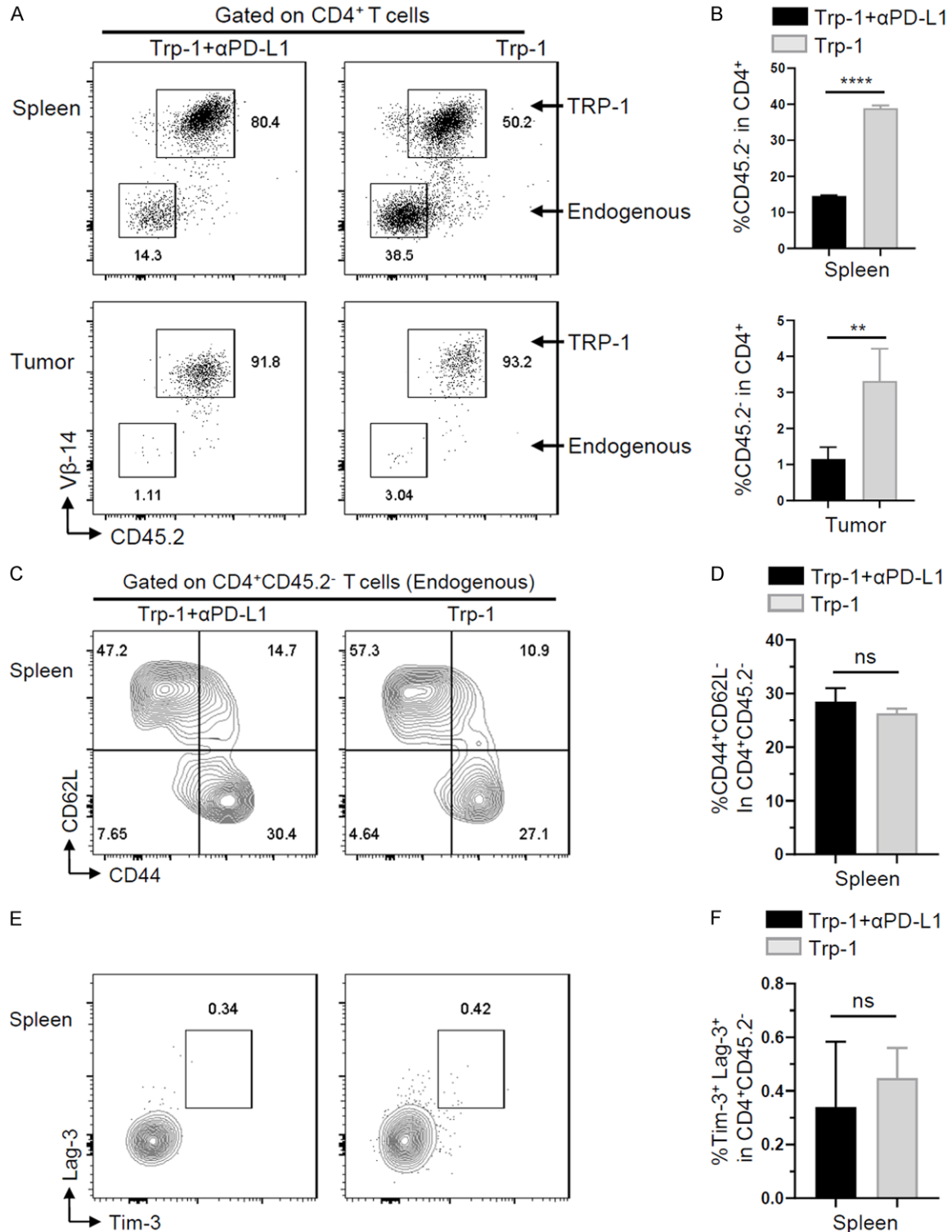
Supplementary Figure 4. Changes of endogenous CD4+ T lymphocytes in response to adoptive transfer of Trp-1 CD4+ T cells and immune checkpoint blockade. A and B. Proportions of endogenous CD4+ T lymphocytes (CD45.2-) among gated total CD4+ T lymphocytes isolated from spleens on day 24. C and D. The percentage of CD62L-CD44+ T lymphocytes among the endogenous CD4+ T lymphocytes in spleens. E and F. Tim-3 and Lag-3 expression on the endogenous CD4+ T lymphocytes in spleens. Data are presented as mean ± SD (n=4). ns: $P>0.05$, *: $P<0.05$, **: $P<0.01$, ***: $P<0.001$, ****: $P<0.0001$.